Young Scientist- Tomorrow's Science Begins Today
Vol. 3, Issue 1 - 2019

EFFICIENT D-Π-A TYPE ORGANIC DYES HAVING CARBAZOLE BASED FUNCTIONAL GROUPS MOIETY AS ACCEPTOR FOR DYE-SENSITIZED SOLAR CELLS: EXPERIMENTAL AND THEORETICAL STUDIES

A VICTOR BASTIN[*], I RAGAVAN[**], PM ANBARASAN[**], A PRAKASAM[***], S MEENAKSHI SUNDAR[*]

ABSTRACT

Two new donor-bridge-acceptor Carbazole with ethyl 2-oxopropanoate, 2-oxopropanoic acid functional group moiety, coded P1 and P2, were synthesized and used as sensitizers in dye sensitized solar cells (DSSCs). The polarizability (α) and first order static hyperpolarizability (β) of P1 and P2 is calculated and the results are discussed. The observed FT-IR and FT-Raman data have been compared with computed frequencies and molecular electrostatic potential map approach have calculated by DFT method. Both dyes showed excellent photovoltaic properties with power conversion efficiency values of 6.72 and 6.40% for P1 and P2 respectively.

KEYWORDS: Dye-Sensitized Solar Cells (Dsscs), Optical And Electrochemical Properties, I-V Characterization, MEP.

INTRODUCTION

Solar energy, as a clean and continual energy resource, supplies sustainable developments of our society. The directly efficient utilization of solar energy is mainly realized by plants expect for photovoltaic power stations and photo-thermal instruments. Along with the development of human society, the contradiction between the production and require of energy becomes more and more severe. Accordingly and in view of the environmental and economic issues of photovoltaic fabrications, dye-sensitized solar cells (DSSCs) have been expected as a potential alternative to conventional inorganic solid state solar cells in terms of their low costs, flexibility and easy manufacturing processes [1-5]. In DSSCs, dyes play pivotal roles since it governs the photon harvesting and the charge generation as well as separation [6,7]. Although metal-containing dyes, such as polypyridylRu(II) and porphyrinZn photosensitizers, have shown excellent photovoltaic performance, [8-13] the limited resources and complicated syntheses restrain their application in large scales [14-16]. In comparison, the metal-free organic dyes with donor-π-acceptor (D-π-A) structure present promising development potential in view of their

[*]Department of Physics, Sri Paramakalyani College in Alwarkuichi, MS University, Tirunelveli, India.
[**]Department of Physics, Periyar University, Salem - 636 011, India.
[***]Department of Physics, Thiruvalluvar Government arts college, Rasipuram, Namakkal – 637 401, India.
Correspondence E-mail Id: editor@eurekajournals.com

 ISSN: 2581-4737

comparably high efficiency, low cost, as well as easier preparation and purification [17-23] Since Sun and co-authors reported their metal-free organic dye T2-1, phenothiazine (PTZ) has become a well-known electron-rich skeleton in photosensitizers [24]. These dyes were then modified by various electron-donating groups, in which, the dyes possessing a structural feature of direct linkage between additional electron donor and PTZ showed worse photovoltaic performance in their DSSC devices [25-27]. It is of large importance to understand the property of the electron donor groups on the chemical stability, electron transfer properties, light-harvesting as well as their joint contribution to the Building Integrated photovoltaic devices.

Recently, Bhanumathi Nagarajan and co-adsorbents [28] are reported to result in Six new class of dyes phenothiazine based on π-conjugated moiety are synthesized and analyzed. In metal-free Dye-sensitized solar cells are devices fabricated using these dyes with and without co-adsorbent, chenodeoxychloicacid. The molecular modeling approximately the phenothiazine moiety enabled a maximum of 12 % photoconversion efficiency with one of the dyes.Zhu and co-authors have reported various organic dyes with a new structure of D-A-π-A, in which, benzothiadiazoles were introduced between electron donor and π-bridge moieties as an electron acceptor [29□32]. Similar structural dyes of D-A-π-A with quinoxaline, benzotriazole and phthalimide as new electron acceptors were also reported lately [33-41]. These additional electron acceptors can be regarded as “electron trap” tools that can modulate the molecular energy gap, broaden the light-harvesting range and promote the electron transfer from donor to anchor [29].

We have reported carbazole-based D-π-A dyes of P1 and P2, in which π-spacers facilitate intramolecular charge separation via interrupting the conjugation of the electron donors. The theoretical and modeling scientists are taking interest in purpose of the Molecular structural, electronic and vibration spectral properties of the title compounds. These new dyes especially dye P1 display a notably enhanced power conversion efficiency of 6.72%, which is superior to the performance of the basic D–π–A dye P2 (6.40%). Finally, these novel dyes have been successfully used as sensitizers to the nanocrystalline TiO_2 based DSSCs and their improved performances and employ the corresponding devices for photovoltaic characteristics are also been presented.

EXPERIMENTAL SECTION

All solvents and reagents were purchased from Alfa-Asear Company and used as received without further purification. **Ethyl 2-(5-(2-(9H-carbazol-9-yl) acridin-6-yl) thiophen-3-yl)-2-oxoacetate (P1):**To a 50 mL round flask were added Carbazol (2.0 g, 11.96 mmol), 3,5a-dihydro-2H-phenothiazine (1.7 mL, 12.5 mmol) and Ethyl 2-oxo-2-(thiophen-3-yl) acetate (0.6 ml)was added and the reaction mixture was heated to 60^0C for 8h .After the addition, the reaction mixture was allowed to stir at room temperature for 12 h.It was crystallized from dichloromethane mixture to obtain the pure sample. ^{1}H NMR□: 10.778738ppm (0.12cm), 11.2677 (0.20), 9.371016ppm (2.51cm), 8.984582 ppm (2.51cm), 8.984582ppm (0.11cm), 8.584347 ppm (0.11cm), 8.8198 (0.13), 8.584347ppm (0.00cm), 8.446335ppm (0.00cm), 8.5338 (0.01), 8.446335ppm (2.51cm), 8.294522ppm (2.51cm), 8.294522ppm (0.02cm), 8.170311ppm (0.02cm), 8.1971 (0.02), 8.059901ppm (2.51cm), 7.783877 ppm (2.51cm), 7.9596 (3.88), 7.783877ppm (0.02cm), 7.659667 ppm (0.02cm), 7.7162 (0.02), 7.659667ppm (0.08cm), 6.224342ppm (0.08cm), 3.698722ppm (2.62cm), 3.339891ppm (2.62cm), 3.5333 (3.10), 3.091469ppm (0.11cm), 2.925855 ppm (0.11cm), 3.0325 (0.11), 2.925855ppm (7.01cm).

2-(5-(3-(9H-carbazol-9-yl)-3,5a-dihydro-2H-phenothiazin-8-yl)thiophen-3-yl)-2-oxoacetic

 ISSN: 2581-4737

acid (P2):A procedure similar to that used for P1 was followed reaction of 3,5a-dihydro-2H-phenothiazine (1.246 g), 3,5a-dihydro-2H-phenothiazine (0.58 g), 2-oxo-2-(thiophen-3-yl) acetic acid (0.6 ml)was added drop wise into the reaction mixture at 0^{o}C are shown in Scheme 1. ^{1}H NMR: 7.3653 (0.26), 7.4560 (0.25), 6.2434 (0.27), 6.0887 (0.54), 4.8583 (0.04), 3.3786 (0.16), 3.5675 (0.12), 2.9457ppm (14.0.01cm), 2.5240 ppm (14.11cm), 2.9842 (12.01), 2.7632 (10.23), Calculated for ^{1}H NMR: phenothiazine 6.7, 6.8, 6.7, 7.0ppm, 9H-fluorene 7.55, 7.28, 7.38, 7.84, 7.38.

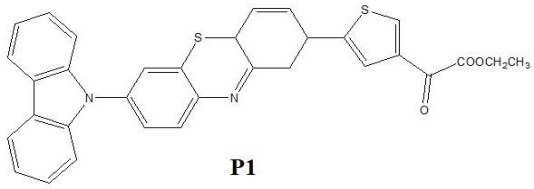

P1

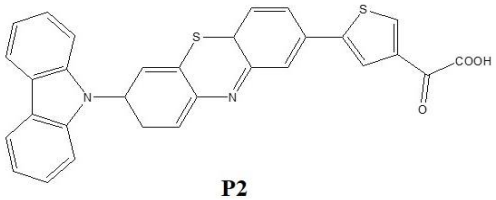

P2

Scheme 1.Synthesis and structure of P1 and P2

The compounds 9H-carbazole, 3,5a-dihydro-2H-phenothiazine, 2-oxo-2-(thiophen-3-yl)acetic acid and Ethyl 2-oxo-2-(thiophen-3-yl) acetate was obtained from Alfa Aesar Chemical Company, India with purity of better than 99% and were used without further purification. The FT-IR spectrum of the ACM was recorded in Ge-based coating on KBr pellet technique using TENSOR27 type a spectrometer in 4000-400 cm-1 region with 0.125 cm^{-1} resolution. The FT-Raman spectra of the [Mn (DDTC) 2] solid sample were measured at room temperature using a Bruker Spectrometer (model LabRAM HR Evolution) in 785nm Wavelength. The excitation light source was a 1064 nm Nd: YAG laser. The solar cell efficiency is determined by its current-voltage (JV) characteristics under standard illumination conditions (Keithley, model 2400). A standard solar spectrum of air mass 1.5 (AM 1.5) with an intensity of 100 W/m^{2} also referred to as 1 sun, is used for solar cell characterization. The AM 1.5 spectrum corresponds to sunlight that has path through the atmosphere 1.5 times longer than when the sun is directly overhead.

COMPUTATIONAL METHODS

The Molecular structure of P1 and P2 dyes have been completely optimized without any equilibrium constraints at the B3LYP method of DFT at 6-31g (d) level theory using Gaussian 09 series of programs. The time-dependent DFT (TD-DFT) calculation containing solvation effect of DMSO is good performed on the optimized methods with the B3LYP functional approach associated with the conductor-like polarizable continuum model (CPCM) [42-44] is conducted employing parameters and the molecular electrostatic potential (MEP) analyzed.

RESULT AND DISCUSSION

MOLECULAR GEOMETRY

The optimized geometry of the P1 and P2 dyes is shown in Figure 1. The optimized geometrical parameters obtained by the large basis set calculation, the bond lengths, bond angles and dihedral angles are listed in Table 1. Since the molecular structure of P1 and P2 compounds of

 ISSN: 2581-4737

the simulated values we can find that most of the optimized bond lengths, bond angles and dihedral angles. The distance between C30-C33, C33-C34 and C21-C22, C22-O23, C22-O24 atoms in cyanine groups of P1 and P2 dyes are 1.3676, 1. 3471 and 1. 3968, 1.3652, 1.3998 Å respectively at B3LYP/6-311++G (d, p).

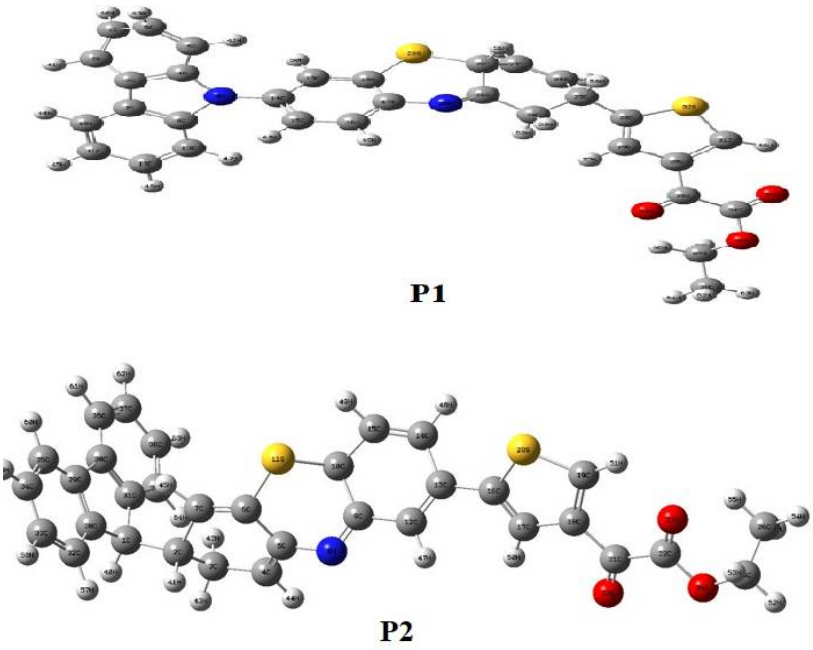

Figure 1

Table 1.The selected bond length (angstrom), bond angle (degree) and dihedral angle (degree) of the dyes P1and P2

Dye	Bond length(Å)		Bond Angle(°)		Dihedral Angle (°)	
P1	C30-C33	1.3676	C30-C33-O39	124.0093	C30-C33-C34-O36	-170.035
	C33-C34	1. 3471	C33-C34-O35	124.0115	O39-C33-C34-O36	-144.011
			C33-C34-O36	132.991	O35-C34-O36-C37	-178.284
			C34-O36-C37	118.0066	O36-C37-C38-H62	-179.961
P2	C21-C22	1. 3968	C18-C21-O27	126.0033	C18-C21-C22-O24	-180.0103
	C22-O23	1.3652	C18-C21-C22	126.9989	C22-O24-C25-C26	180.3079
	C22-O24	1.3998	C22-O24-C25	114.0038	H53-C25-C26-H55	-179.0239
			O24-C25-C26	113.1473	C22-O24-C25-H52	-157.0052

OPTICAL AND ELECTROCHEMICAL PROPERTIES

The absorption spectra of P1 and P2 in dichloromethane (CH_2Cl_2) solution and the computed absorption spectrum are shown in Figure 2 and their relative intensities are tabulated in Table 2. The variation of the π-bridge of the electron- donating moiety leads to significant changes in the position of the lowest energy absorption band. The Calculated intramolecular charge transfer (ICT) absorption peak in the visible region is observed at λ_{max} = 584 and 530 nm for P1 and P2, respectively. As listed in Table 2, when replacing the thiophene unit with acid group acceptor, the absorption spectra of P1 and P2 broaden with respect to P1 in the visible region, and the absorption peaks (λ_{max}) are red shifted by 395 and 382, 460 nm, respectively.

Optimized Molecular Structure of P1 and P2

 ISSN: 2581-4737

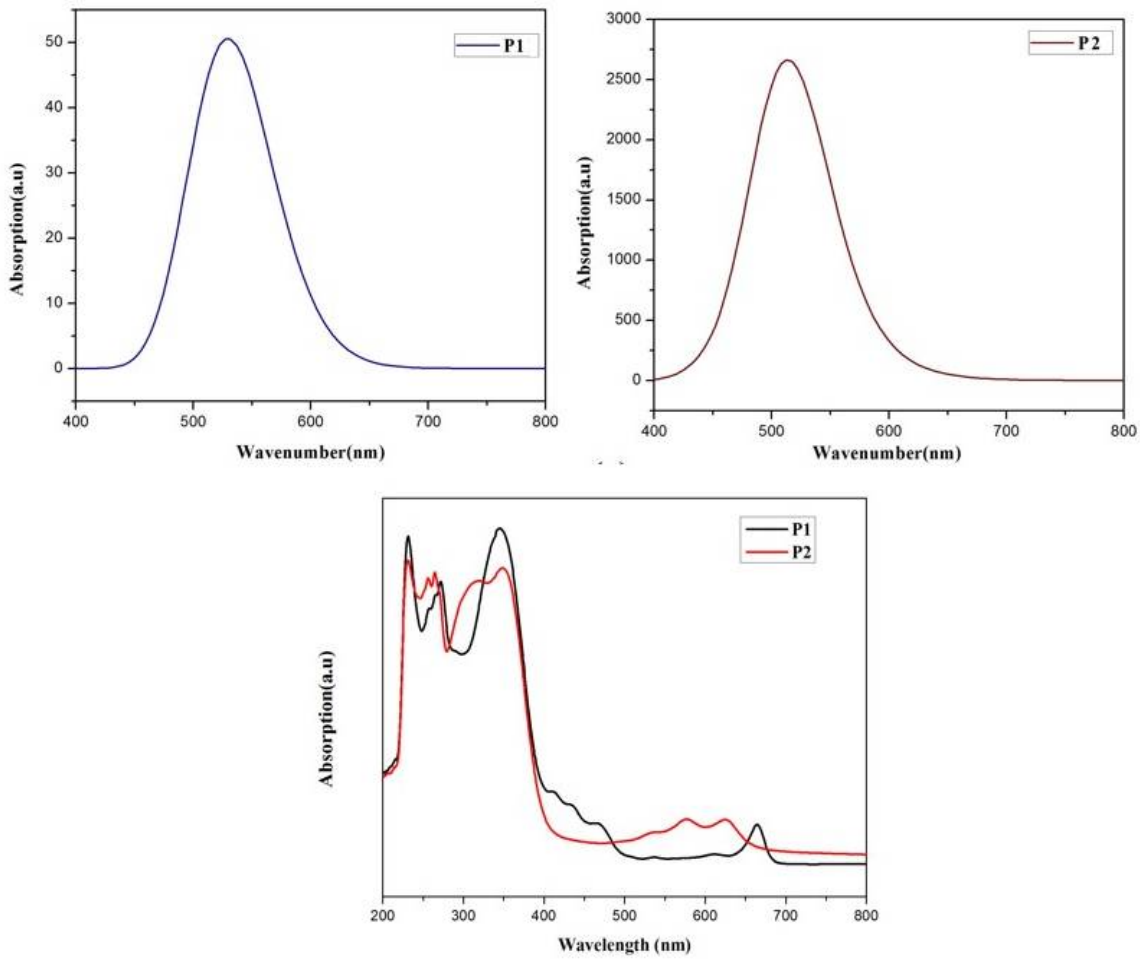

Figure 2 Experimental and Simulated UV-Vis spectra of P1 and P2

Table 2.Absorption wavelength (in nm), oscillator strength (f in a.u.), orbital transitions and light harvesting efficiency (LHE) of the dyes P1 and P2

Mol.	Energy (cm^{-1})	Wavelength (nm)	Osc. Strength	Major contribs	Minor contribs	LHE
P1	18848	584	0.0005	H->L (97%)		-.0.00115
	19023	525	0.0028	H-6->L (66%), H-5->L (25%)	H-8->L (4%)	-0.00646
	20374	490	0.0034	H-2->L (96%)	H-1->L (3%)	-0.00785
P2	17098	530	0.0013	H->L (99%)		-0.00299
	19469	513	0.0362	H->L+1 (94%)	H-1->L+1 (2%)	-0.08692
	21923	456	0.0023	H-6->L (22%), H-1->L (52%)	H-8->L (17%), H-2->L (6%)	-0.00530

The electrochemical properties of P1 and P2 dyes were determined by using cyclic voltammetry (CV) with the aim to obtain the energy level position of the frontier or bitals. Under the application of positive potential, CV showed two quasi reversible oxidation waves which correspond to an oxidation-reduction process. These two peaks observed at ($E_{1/2}^{ox}$) at -1.80, 2.43 V for P1 (-1.75 V and 1.67 V for P2) versus ferrocene/ ferrocenium (Fc/Fc +) are attributed

 ISSN: 2581-4737

to the oxidation of π-conjugated backbone and carbazole donor respectively. The well-defined first oxidation peak for P2 compared to P1, confirms better charge transfer between D-π-A in case of ethyl 2-oxopropanoate compared to the 2-oxopropanoic acid. The HOMO and LUMO levels of P1 and P2 compounds were determined from the spectral analysis and CV data which are summarized in Table. We have also recorded CV of the cobalt based redox shuttle in order to find out the electrochemical potentials and energy level of the same (Figure 3).

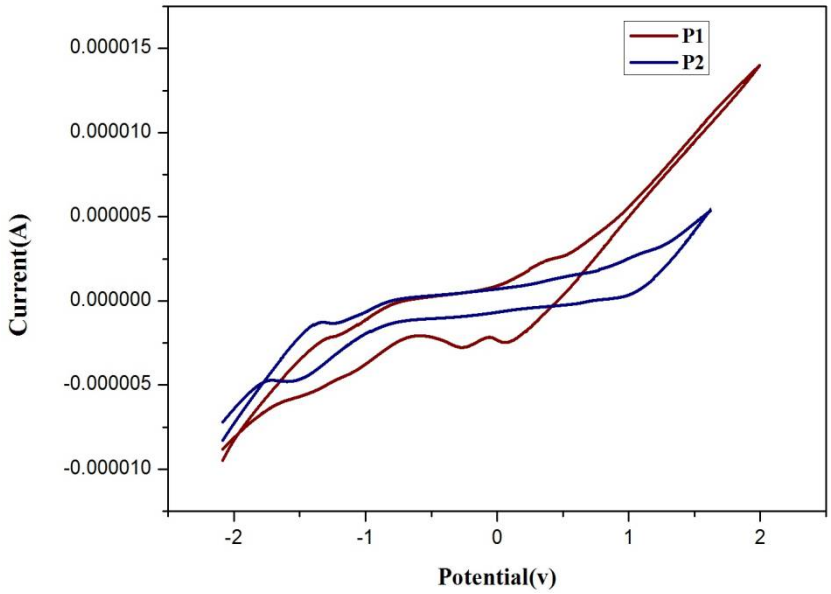

Figure 3.Cyclic Voltammograms of solid electrolytes

VIBRATIONAL ANALYSIS

The geometry of the molecule is possessing Cs point group symmetry. The 80 normal modes of vibrations are span into 51 modes of vibrations are in-plane bending vibrations of A' and 29 modes of vibrations are out of plane bending of modes A'' species. The experimental FT-IR and FT-Raman spectra of the title compounds along with the computed spectra are shown in Figs. 4 and 5. The observed FT-IR and FT-Raman wavenumbers along with the theoretical infrared and Raman frequencies of alongwith their relative intensities and probable assignments. The Benzene or aromatic ring C-H stretching vibration modes usually occurs in the region 3100 and 3000 cm^{-1}. In general, the bands are not affected significantly by the environment of substituents. The C-H aromatic stretching vibrations are present in the benzene ring of P1 and P2 are seen as weak bands at 3086 and 3012 cm^{-1}. The C-H aromatic in-plane vibration modes of hexagon ring and its derivatives are normally found between 1300–1000 cm^{-1}. The prominent absorption peaks at 1153 and 1131 cm^{-1} in IR are assigned to the C-H aromatic in-plane bending vibration frequencies and C-H out of plane bending vibration frequencies of aromatic ring are observed in the region 1100–600 cm^{-1}. The aromatic C-H out of plane bending vibrations of P1 and P2 is seen in the infrared spectrum at 704, 642 and 561 $cm^{-1}$and in the Raman spectrum at 715 and 583 cm^{-1}. The ring carbon–carbon stretching vibrations occur in the region 1625–1430 cm^{-1}. For benzene six-membered rings, e.g., pyridines and aromatic, there are two or three vibration modes in this region due to skeletal vibrations, the strongest usually being at about 1512 cm^{-1}. Chithambarathanu et al. [45] have observed the FT-IR bands at 1501, 1486 and 1457 cm^{-1} in P1. The aromatic C-C stretching is not observed for the title compound, while the DFT calculations give the aromatic C-C stretching modes at 1309, 1483, 1449, 1530 cm^{-1}.

 ISSN: 2581-4737

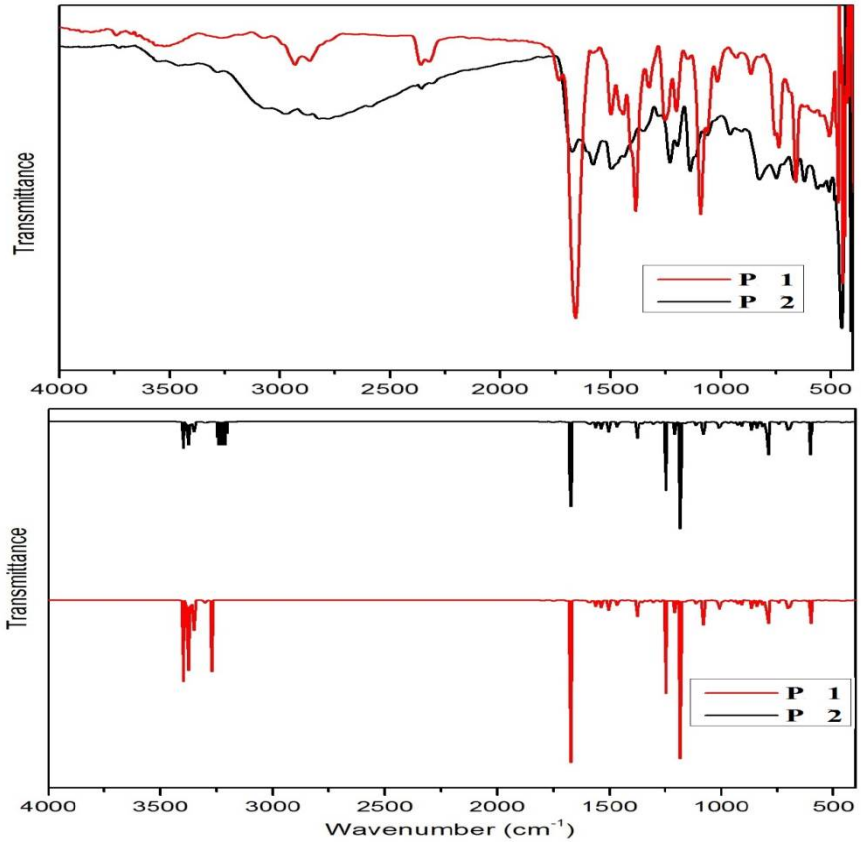

Figure 4.Experimental and theoretical FT-IR spectra of P1 and P2

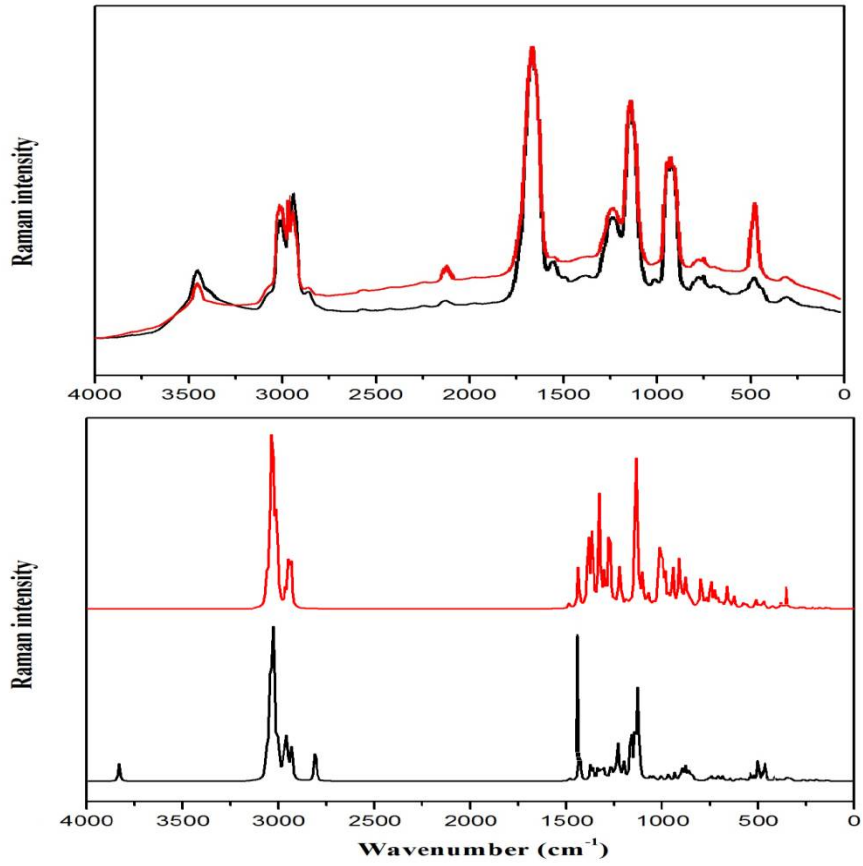

Figure 5.Experimental and theoretical FT-Raman spectra of P1 and P2

 ISSN: 2581-4737

HOMO-LUMO ANALYSIS

In HOMO-LUMO and optical properties, it is essential to examine the HOMOs, LUMOs, energy gaps and oscillator strength. To gain insight into the molecular structures and electron distribution, the geometries of the 9H-carbazole, 9H-fluorene containing H-phenothiazine unit were fully optimized and the density functional theory calculations was carried out employing the B3LYP/6-31G level with Gaussian 09 programme package. Effect of the solvents was simulated by employing DFT calculations using the polarizable continuum model (PCM). As shown in Figure 6, for the zeroth generation 1, 2, 5 and 6 the excited state LUMO was only localized on a heterocyclic ring and also self-charge transfer by the H-phenothiazine group is observed [46, 47]. From the HOMO level of the zeroth generation dendrimers 1, 2, 5 and 6, electron density is homogeneously distributed on the electron donor 9H-carbazole, 3,5a-dihydro-2H-phenothiazine and thiazole as linker system.

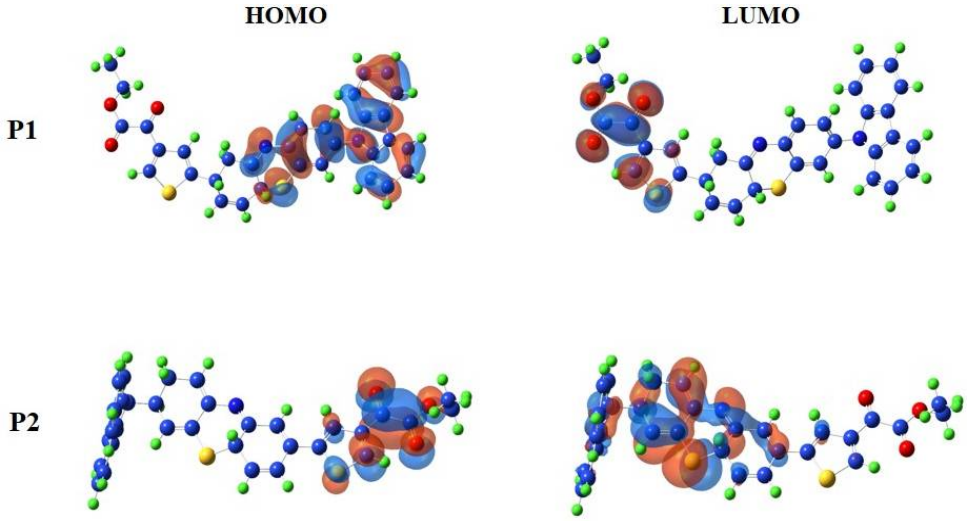

Figure 6.Frontier molecular orbitals of P1 and SP2 dyes

However in the case of dyes 1 and 2, the electron density is distributed to the withdrawing group of phenyl ring due to the conjugation between the phenyl rings in the core unit. It may imply that the planar H-phenothiazine blocked by triphenylamine can make electron distribution of HOMO to the electron distribution of the LUMO. The well overlapped HOMO and LUMO orbitals on the linker thiazine unit suggest the inductive or withdrawing electron tendency from 9H-carbazole, 9H-fluorene donor unit to the H-phenothiazine-based unit. Thus, the HOMO and LUMO energy gap induced by light irradiation could move the excited electron distribution or charge transfer across the thiazine bridge from donor unit to the acceptor unit. The oscillator strength can also prove the charge transfer from donor to the periphery and the oscillator strength, excitation energy values support this observation. The frontier molecular orbital of the zeroth generation dendrimers reveals that HOMO-LUMO excitation moves the electron density distribution from the donor triphenylamine to the acceptor thiophene at the periphery through thiazine bridging unit (Table 3).

Table 3.The HOMO and LUMO energy in eV obtained in B3LYP/6-311++G (d, p)

Dye	HOMO (eV)	LUMO (eV)	Band Gap (eV)
P1	-5.92	-3.34	2.58
P2	-6.35	-3.42	2.93

 ISSN: 2581-4737

POLARIZABILITY AND HYPERPOLARIZABILITY

The calculated and first-order molecular characterize the reaction of a molecular system in an applied electric field [48], and the computational approach allows the determine not only the strength of molecular interactions as well as the cross sections of different scattering and collision processes, but also the molecular nonlinear optical properties (NLO) has been of great interest [40, 41]. In the recent years, because of potential applications in dye sensitizer hemicyanine system, which is the measure of the high NLO property, generally possesses high photocurrent performance. In order to study the relationships among optical signal processing, photoelectric generation, and electronic communication, the polarizabilities and first hyperpolarizabilities of P1 and P2 dyes was calculated.

In addition, the μ_{tot} and β_{tot} of P1 and P2 were also calculated by B3LYP/6-311++G (d, p) level. And the values for μ_{tot} and β_{tot} are 2.4123 D, 2.3529 D and 67.20965 esu, 70.6497 esu shows in Table 4 and 5. This shows that the title compound is a better candidate than P1 and P2. The non-linear optical activity of the molecular system, which is associated with the intramolecular charge transfer, resulting from the electron cloud movement through π conjugated frame work of electron. The physical properties of these conjugated molecular systems are governed by the high degree of molecular charge transfer axis and by the short band gaps.

Table 4.Polarizability (α) of the dyes P1 and P2 (in a.u.)

Dye	P1	P2
α_{xx}	268.8093	203.9407
α_{yy}	217.8628	228.7335
α_{zz}	242.4163	231.9104
α	243.029	221.5282
Δα	113.418	418.65
μ_{tot}	2.4123	2.3529

Table 5.Hyperpolarizability (β) of the dyes P1 and P2 (in a.u.)

Dye	P1	P2
β_{xxx}	549.2194	717.0824
β_{xxy}	77.2177	7.1115
β_{yyy}	57.6503	11.6078
β_{xxz}	36.2551	74.2187
β_{yyz}	-7.3143	15.2356
β_{xzz}	-64.0669	-67.2639
β_{yzz}	3.4629	-1.0940
β_{zzz}	11.6203	-4.0497
β_{tot}	67.20965	70.6497

MOLECULAR ELECTROSTATIC POTENTIAL ANALYSIS

The Molecular electrostatic potential surface is the tool which is used mostly for predicting sites and comparative reactivities towards electrophilic attack of electric point like reagents on organic molecules and molecular properties of small molecules, hydrogen bonding interactions, actions of dye molecules and their analogues [49, 50]. Electrostatic potential map illustrates the charge distributions of the molecule three

 ISSN: 2581-4737

dimensionally. Knowledge of the charge distribution of MEP is in fact responsible for the chemical active behaviour of an agent in a chemical reaction of the molecule. They strongly influence the binding of a substrate to its active site. The Different colors on the MEP surface map are represented by different colors; the red represents regions of the most negative potential, the blue represents regions of the most positive potential surface and the green represents regions of zero potential. The electrostatic potential surface is plotted for title compounds at the B3LYP/6-311++G (d, p), optimized geometry was calculated. The visual presentation of chemical activity, the most positive potential (blue) regions of surface maps are linked to electrophilic attack and the most negative (red) potential is located at the oxygen atom of nitro group which can be considered as possible sites for nucleophilic reactivity as shown in Figure 7**.** It can be seen since the surface maps of the present dyes that the negative potential regions are mainly located at the O and N atoms.

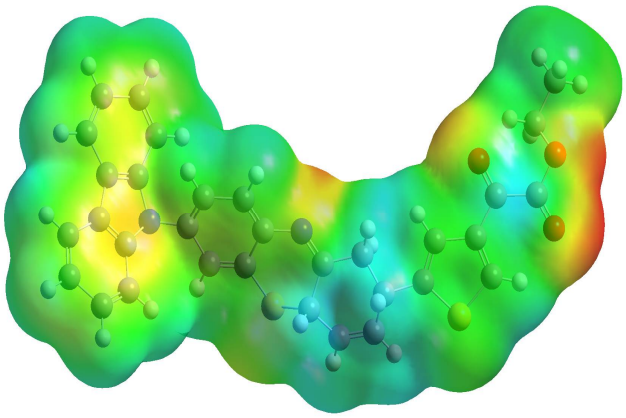

P1

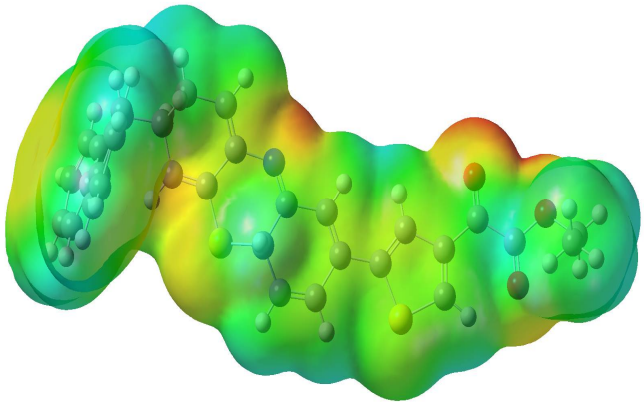

P2

Figure 7.Molecular Electrostatic Potential Surface map of P1 and P2

SEM ANALYSIS

The recorded SEM images of the sample are as shown in Figure8 which provides direct information about the size and typical morphology of the as synthesized powders. The particles appear to be several microstructures, but the magnified representation shows that the agglomerates consisted of tiny crystallites with few tens of nanometer in size. A set of pores and voids were also practical in the agglomerates, which May be caused by the gases released during the combustion process.

 ISSN: 2581-4737

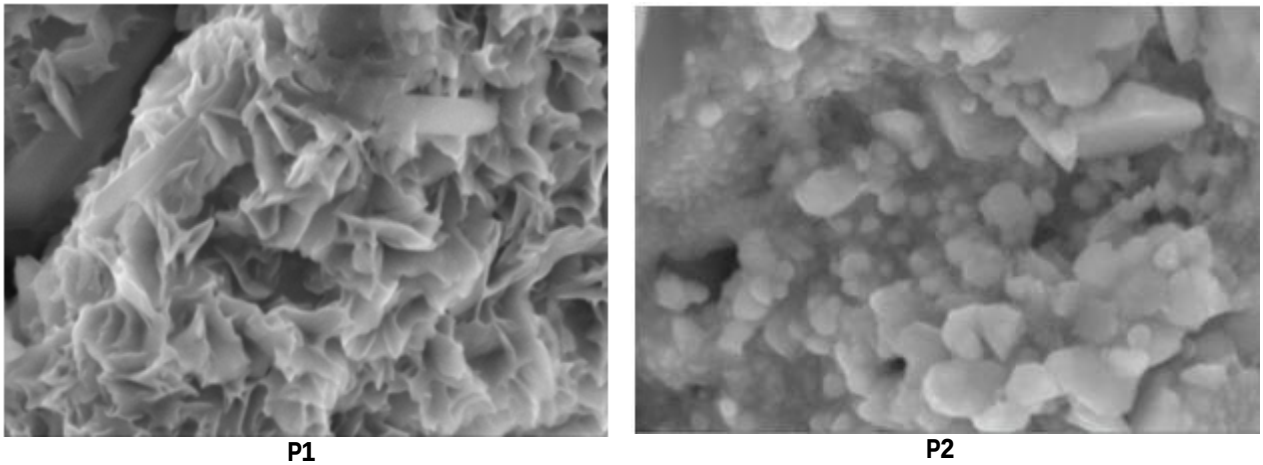

P1 **P2**

Figure 8.SEM images of with P1 and P2 dyes

I-V CHARACTERIZATION

The photovoltaic parameters for the constructed solar energy conversion are analyzed by employing the sensitizers in DSSC. We first studied the effects of dye adsorption solvent based on the P1 and P2 dyes shown in **Table 6**. The overall conversion efficiencies η were derived from the equation $\eta = J_{sc}V_{oc}FF$, where Jsc is the short circuit current density, Voc is the open circuit voltage, and FF is the fill factor. The photocurrent density–photovoltage (*J*–*V*) curves of sensitizers with solvent based measured under simulated AM 1.5 solar irradiation (100 mW cm^{-2}) are depicted in Figure 9. The resulting P1 and P2 dyes present the higher dye uptake amount produces the larger J_{sc}. The best performances are achieved with the J_{sc} of 12.3 mA/cm^2, V_{oc} of 0.79, Efficiency (η) 6.72% by P1 as the dye adsorption solvent.

Table 6.Photovoltaic performance of the dyes

Dye	V_{oc} / V(mV)	J_{sc} (mA/cm^2)	Efficiency (η in %)
P1	0.79±0.003	12.3	6.72
P2	0.79±0.003	12.0	6.40

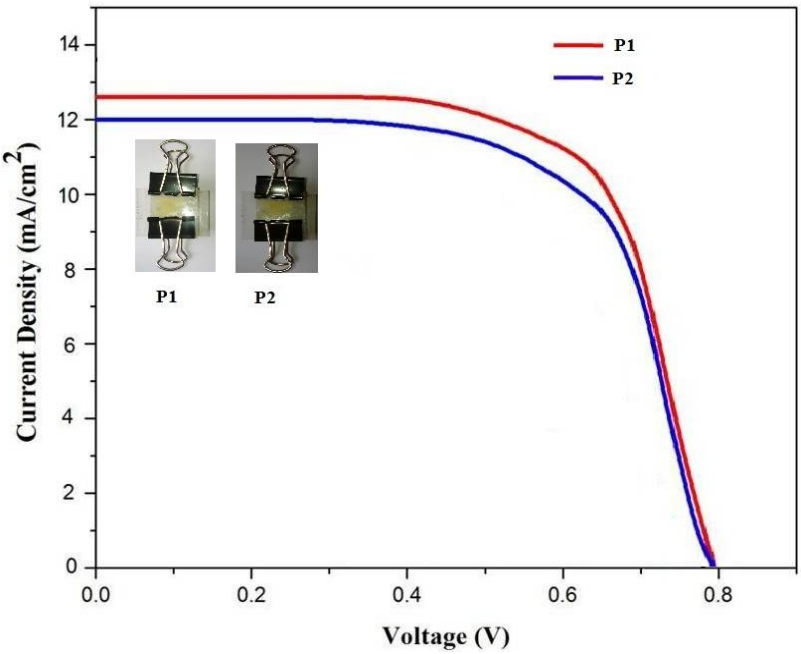

Figure 9.Short-circuit photocurrent density–voltage (Jsc–V) curve for the fabricated device with P1 and P2 dyes

 ISSN: 2581-4737

CONCLUSION

In conclusion, we have demonstrated a design strategy and synthesis of novel D–π–A type organic sensitizers different functional groups modifications that will optimize the photovoltaic properties of the carbazole-based DSSCs. We use this theoretical procedure to gain insights into the Molecular structure and electronic structures of the dyes. The Vibrational spectra and electronic transitions computed by a TD-DFT method including P1 relativistic effects show good agreement with the experimental data. In the spectroscopy signature region, both the IR and Raman peaks are found to have large intensities, which reflects large changes in the molecular dipole moment and molecular polarizability. Also, the vibrational contribution to NLO activity has been proposed.

Photovoltaic measurements of the corresponding DSSCs showed an enhanced photovoltaic performance for the P1 sensitized solar cell, as a result of its higher short circuit current J_{sc} and open circuit voltage V_{oc} parameters. Additionally, their HOMO-LUMO energy levels are in good alignment with that of P1 dye rendering them suitable for use in solid-state dye-sensitized solar cell and Molecular electrostatic potential were analyzed. It is likely that the introduction of the additional anchoring group extended the conjugation of the dyes between the electron donor and electron acceptors into the carbazole structure will further improve the performance of DSSCs.

ACKNOWLEDGEMENTS

The authors are thankful to the learned referees for their useful and critical comments, which improved the quality of the manuscript. The theoretical study was supported by the Nano and Hybrid Materials Laboratory, Periyar University, Salem-11.

REFERENCES

[1.] B. O'Regan and M. Grätzel, *Nature* 1991, 353, 740.

[2.] U. Bach, D. Lupo, P. Comte, J. E. Moser, F. Weissörtel, J. Salbeck, H. Spreitzer and M. Grätzel, *Nature* 1998, 395 ,585.

[3.] L. Pan, J. Zou, X. Zhang, L. Wang, *J. Am. Soc. Chem.* 2011, 133,10002

[4.] J. H. Yum, E. Baranoff, F. Kessler, T. Moehl, S. Ahmad, T. Bessho, A. Marchioro, E. Ghadiri, J. E. Moser, C. Yi, M. K. Nazeeruddin and M. Grätzel, *Nat. Commun*. 2012, 3,638.

[5.] A. Hagfeldt, G. Boschloo, L. Sun, L. Kloo and H. Pettersson, *Chem. Rev*. 2010, 110 , 6663.

[6.] M. Grätzel and S. M. Zakeeruddin, *Mater. Today* 2013, 16,18.

[7.] T. Mohr, V. Aroulmoji, R. S. Ravindran, M. Muller, S. Ranjitha, G. Rajarajan and P. M. Anbarasan, *Spectrochim. Acta. A* 2015, 135, 1073.

[8.] L. E. Polander, A. Yella, B. F. E. Curchod, N. Ashari Astani, J. Teuscher, R. Scopelliti, P. Gao, S. Mathew, J.-E. Moser, I. Tavernelli, U. Rothlisberger, M. Grtzel, M. K. Nazeeruddin and J. Frey, Angew. *Chem. Int. Ed*. 2013, 52, 8735.

[9.] M. K. Nazeeruddin, F. De Angelis, S. Fantacci, A. Selloni, G. Viscardi, P. Liska, S. Ito, B. Takeru and M. Grätzel, *J. Am. Chem. Soc*. 2005, 127, −16847.

[10.] A. Yella, H. Lee, H. N. Tsao, C. Yi, A. K. Chandiran, M. K. Nazeeruddin, E. W. Diau, C. Yeh, S. M. Zakeeruddin and M. Grätzel, *Science* 2011, 334 , 634.

[11.] S. Mathew, A. Yella, P. Gao, R. Humphry-Baker, B. F. E. Curchod, N. Ashari-Astani, I. Tavernelli, U. Rothlisberger, M. K. Nazeeruddi and M. Grätzel, *Nat. Chem*. 2014, 6, 247.

[12.] F. Gou, X. Jiang, B. Li, H. Jing and Z. Zhu, *ACS Appl. Mater. Interfaces* 2013, 5, 12637.

[13.] F. Gou, X. Jiang, R. Fang, H. Jing and Z. Zhu, *ACS Appl. Mater. Interfaces* 2014, 6, 6703.

 ISSN: 2581-4737

[14.] W. Zeng, Y. Cao, Y. Bai, Y. Wang, Y. Shi, M, Zhang, F. Wang, C. Pan and P. Wang, *Chem. Mater*. 2010, 22, 1925.

[15.] J. H. Delcamp, A. Yella, T. W. Holcombe, M. K. Nazeeruddin and M. Grätzel, *Angew. Chem.* 2013, 52, 380.

[16.] L. Han, A. Islam, H. Chen, C. Malapaka, B. Chiranjeevi, S. Zhang, X. Yang and M. Yanagida, *Ener. Environ. Sci*. 2012, 5, 6060.

[17.] Z. Fang, A. A. Eshbaugh and K. S. Schanze, *J. Am. Chem. Soc*. 2011, 133 , 3069.

[18.] Y. Wu, X. Zhang, W. Li, Z. Wang, H. Tian and W. Zhu, *Adv. Energy Mater*. 2012, 2, 156.

[19.] Y. Hua, L. T. L. Lee, C. Zhang, J. Zhao, T. Chen, W. Y. Wong, W. K. Wong and X. Zhu, *J. Mater. Chem. A* 2015, 3, 13855.

[20.] X. Ren, S. Jiang, M. Cha, G. Zhou and Z. Wang, Chem. Mater. , 2012, 24, 3499.

[21.] Y. Hua, B. Jin, H. Wang, X. Zhu, W. Wu, M. Cheung, Z. Lin, W. Y. Wong and W. K. Wong, *J. Power Source*, 2013, 237 , 203.

[22.] Y. Ooyama and Y. Harima, *Chem. Phys. Chem.* 2012, 13, 4080.

[23.] S. Kim, J. K. Lee, S. O. Kang, J. Ko, J.-H. Yum, S. Fantacci, F. De Angelis, D. Di Censo, M. K. Nazeeruddin and M. Grätzel, *J. Am. Chem. Soc*. 2006, 128 , 16707.

[24.] H. Tian, X. Yang, R. Chen, Y. Pan, L. Li, A. Hagfeldt and L. Sun, *Chem. Commun.* 2007, 3743.

[25.] S. Wang, H. Wang, J. Guo, H. Tang and J. Zhao, *Dyes Pigm.* 2014, 109, 96□104.

[26.] Y. Lin, B. Ke, Y. Chang, P. Chou, K. Liau, C. Liu and T. J. Chow, *J. Mater. Chem. A* 2015, 3, 16842.

[27.] Y. Hua, S. Chang, D. Huang, X. Zhou, X. Zhu, J. Zhao, T. Chen, W. Y. Wong and W. K. Wong, *Chem. Mater*. 2013, 25, 2153.

[28.] N. Bhanumathi, S. kushwaha, R. Elumalai, S. Mandal, K. Ramanujam and D. Raghavachari, *J. Mater. Chem. A* 2017.

[29.] Y. Wu and W. Zhu, *Chem. Soc. Rev*. 2013, 42, 2058.

[30.] W. Zhu, Y. Wu, S. Wang, W. Li, X. Li, J. Chen, Z. Wang and H. Tian, Adv. Funct. Mater., 2011, 21, 763.

[31.] H. Zhu, W. Li, Y. Wu, B. Liu, S. Zhu, X. Li, H. Ågren and W. Zhu, ACS Sustainable *Chem. Eng*. 2014, 2, 1034.

[32.] B. Liu, F. Giordano, K. Pei, J. D. Decoppet, W. Zhu, S. M. Zakeeruddin and M. Grätzel, *J. Chem. Eur*. 2015, 21 , 18661.

[33.] K. Pei, Y. Wu, W. Wu, Q. Zhang, B. Chen, H. Tian and W. Zhu, *J. Chem. Eur*. 2012, 18 , 8200.

[34.] X. Li, S. Cui, D. Wang, Y. Zhou, H. Zhou, Y. Hu, J. Liu, Y. Long, W. Wu, J. Hua and H. Tian, *Chem. Sus. Chem*. 2014, 7, 2888.

[35.] D. Chang, H. Lee, J. Kim, S. Park, S. Park, L. Dai and J. Baek, *Org. Lett*. 2011, 13, 3883.

[36.] Y. Cui, Y. Wu, X. Lu, X. Zhang, G. Zhou, F. B. Miapeh, W. Zhu and Z. Wang, *Chem. Mater.* 2011, 23, 4401.

[37.] J. Liu, B. Liu, Y. Tang, W. Zhang, W. Wu, Y. Xie and W. Zhu, *J. Mater. Chem. C* 2015, 3, 11150.

[38.] X. Hu, S. Cai, G. Tian, X. Li, J. Su and J. Li, *RSC Adv*. 2013, 3, 22553.

[39.] W. Li, Y. Wu, Q. Zhang, H. Tian and W. Zhu, *ACS Appl. Mater. Interfaces* 2012, 4, 1830.

[40.] A. D. Hendsbee, S. M. McAfee, J. Sun, T. M. McCormick, I. G. Hill and G. C. Welch, *J. Mater. Chem. C* 2015, 3, 8915.

[41.] Z. Huang, C. Cai, X. Zang, Z. Iqbal, H. Zeng, D. Kuang, L. Wang, H. Meierd and D. Cao, *J. Mater. Chem. A* 2015, 3, 1344.

[42.] J. Frisch, G.W. Trucks, H.B. Schlegel, G.E. Scuseria, M.A. Robb, J.R. Cheeseman, H. Nakatsuji, M. Caricato, X. Li, H.P. Hratchian, K. Toyota, R. Fukuda, J. Hasegawa, M. Ishida, R. Nakajima, Y. Honda, O. Kilao, H. Nakai, T. Verven, J.A. Montgomery Jr., J.E. Peralta, F. Ogliaro, M. Bearpark, J.J. Heyd, E. Brothers, K.N. Kudin, V.N. Staroveror, R. Kobayashi, J. Normand, K. Ragavachari, A. Rendell, J.C. Burant, S.J. Tomasi, M. Cossi, N. Rega, J.M. Millam, M. Klene, J.E. Knox, J.B.Cross, V. Bakken, C. Adamo, J. Jaramillo, R. Gomperts, R.E. Strattmann, O.Yazyev, A.J. Austin, R. Cammi, J.W. Ochetrski, R.L.

 ISSN: 2581-4737

Martin, K. Morokuma, V.G. Zakrazawski, G.A. Votn, P. Salvador, J.J. Dannenberg, S. Dapprich, A.D. Daniels, O. Farkas, J.B. Foresman, Gaussian O.G., Revision A.O2, Gaussian Inc., *Wallingford, CT*. 2009.

[43.] V. Barone, M. Cossi, *J. Phys. Chem. A* 1998, 102, 2001.

[44.] M. Cossi, V. Barone, R. Cammi, J. Tomasi, *Chem. Phys. Lett*. 1996, 255, 335.

[45.] T. Chithambarathanu, V. Umayourbaghan, V. Krishnakumar, Indian *J. Pure Appl. Phys.* 2003, 41, 878.

[46.] M. Bakiler, I.V Maslov, S. Akyuz, *J. Mol. Struct*. 1999, 475, 83.

[47.] J.S. Murray, K. Sen, Molecular Electrostatic Potentials, Concepts and Applications, *Elsevier*, *Amsterdam* 1996, 7, 624.

[48.] Y.R Shen, the Principles of Nonlinear Optics, Wiley, New York 1984.

[49.] J.S. Murray, K. Sen, Molecular Electrostatic Potentials, Concepts and Applications, *Elsevier, Amsterdam, Netherlands* 1996.

[50.] E. Scrocco, J. Tomasi, Electronic molecular structure, reactivity and intermolecular forces: Aneuristic interpretation by means of electrostatic molecular potentials. *Adv. Quantum Chem*. 1978, 11, 193.

 ISSN: 2581-4737